PERGAMON

Chemical Engineering Science 56 (2001) 5693–5707

Chemical Engineering Science

www.elsevier.com/locate/ces

Computing radial packing properties from the distribution of particle centers

N. J. Mariani[a,b], O. M. Martínez[a,c], G. F. Barreto[a,c,*]

[a] *Facultad de Ingeniería, Departamento de Ingeniería Química, Universidad Nacional de La Plata, Calle 47 No. 257, CC 59, 1900 La Plata, Argentina*

[b] *Pinmate, Facultad de Ciencias Exactas y Naturales, Departamento de Industrias, Universidad de Buenos Aires, Ciudad Universitaria, Buenos Aires, Argentina*

[c] *Centro de Investigación y Desarrollo en Procesos Catalíticos (CINDECA), CONICET-Universidad Nacional de La Plata, Calle 47 No. 257, CC 59, CP B1900AJK, La Plata, Argentina*

Received 18 October 2000; received in revised form 2 July 2001; accepted 22 July 2001

Abstract

The relationship between the distribution of particle centers in random beds of uniformly sized spheres and radial properties, in particular radial voidage profiles, is undertaken in this work. To this end, closed expressions for six geometrical quantities related to the intersection of spheres with cylindrical surfaces are presented. The relations to compute radial properties are then expressed in terms of those geometrical quantities and it is shown that for realistic types of particle center distribution, the calculations can be carried out without resorting to simplifying assumptions or numerical integration. The significance of radial profiles of particle surface area is also discussed. © 2001 Elsevier Science Ltd. All rights reserved.

Keywords: Voidage profile; Particle distribution; Packed bed structure; Aspect ratio; Particle surface area

1. Introduction

It is well known that particles in random packed beds show a certain degree of order close to the wall of the container. This structure is described from a well defined layer of particles against the wall, with most of the particles contacting the wall, followed by a few other layers progressively losing their identity. Finally, far from the wall, particle accommodation becomes strictly at random.

The bed structure close to the wall gains significance in beds of low aspect ratio ($a = R/R_p$) when this region becomes comparable to the whole cross section of the vessel. For example, it can be expected, and in fact it happens, that the permeability of the bed close to the wall will be different from that in the innermost regions. Also, beds of low aspect ratios are industrially employed when heat should be exchanged between the bed and an external medium, or when mass transfer should be carried out through permeable walls. In these cases, the structure of the bed in the near wall region gives rise to distinct transport properties.

The layered structure near the wall is particularly well defined in beds of spherical particles. The subject has been treated in a number of works (see e.g. Mariani, Mazza, Martínez, & Barreto, 1998, for a recent survey), although in most of them the emphasis was put on the local voidage profiles rather than on the distribution of particle centers.

The radial voidage profiles exhibit the shape of a damped oscillation starting with high values of voidage just at the wall. This shape has been usually modelled by empirical expressions. The knowledge of this profile is obviously important in assessing local flow and transport properties. Nonetheless, if the distribution of particles is known, the radial voidage profile can be unambiguously evaluated. From the description given above, it becomes apparent that the identification of a few layers (say, position and density of particle centers) close to

* Corresponding author. Facultad de Ingeniería, Departamento de Ingeniería Química, Universidad Nacional de La Plata, Calle 47 No. 257, CC 59, 1900 La Plata, Argentina. Tel.: +54-221-4210711; fax: +54-221-4254277.

E-mail address: barreto@quimica.unlp.edu.ar (G. F. Barreto).

PII: S0009-2509(01)00295-0

the wall will suffice for describing the particle distribution in practice. This identification is more valuable than that of the voidage profile. Not only the latter can be derived from the former, but also other properties can be evaluated, as the radial profile of particle surface area. Besides, radial profiles of these properties are associated with a pseudo-continuous description of the solid phase. Instead, if a discrete description is used (i.e. explicitly acknowledging the existence of particle layers), the significance of particle distribution is direct.

Experimental methods to measure voidage profiles have been reviewed by Mariani et al. (1998). The direct measurement of particle center distribution has been undertaken less frequently. Some techniques for this purpose will be briefly described in Section 3. Another example is the procedure employed by Dixon and Welch (1987). The potentiality of X-ray computed tomography (e.g. Toye, Marchot, Crine, Pelsser, & L'Homme, 1998) for this purpose should also be mentioned.

The link between the distribution of particle centers in random beds of uniformly sized spheres and radial properties is undertaken in this work. The local voidage in a given radial zone arises from computing the volume of spheres enclosed in that zone. Similarly, the surface of the spheres will define the solid area exposed in the given zone.

We will first present here a closed formulation for six geometrical quantities resulting from the intersection of a sphere with a cylindrical surface.

Then, it will be formally established how radial properties become related to the distribution of particle centers through some of the geometrical quantities, and it will be shown that for realistic types of particle center distributions the computations of radial properties can be carried out without resorting to geometrical simplifications or numerical integration, by using the expression for the six geometrical quantities.

Previous contributions dealing with particle center distribution and radial voidage profiles are analyzed to show that the relations presented here are able to encompass all the expressions proposed or employed in those works.

Finally, the significance of radial profiles of particle surface area is particularly emphasized, as this property has been seldom employed in bibliography.

2. Definitions of geometrical quantities

For a sphere of radius R_p centered at a distance r_c from the axis of a cylindrical surface of radius r, $V(r,r_c)$ is defined as the volume of the sphere left inside the cylindrical surface.

Similarly, $A(r,r_c)$ is the area of the sphere surface left inside the cylindrical surface.

The partial derivatives of $V(r,r_c)$ and $A(r,r_c)$ with respect to r,

$$S(r,r_c)=\partial V(r,r_c)/\partial r, \tag{1a}$$

$$\mathrm{DA}(r,r_c)=\partial A(r,r_c)/\partial r, \tag{1b}$$

and the integrals

$$\mathrm{Vt}(r,r_c)=2\int_0^{r_c} V(r,s)s\,\mathrm{d}s, \tag{2a}$$

$$\mathrm{At}(r,r_c)=2\int_0^{r_c} A(r,s)s\,\mathrm{d}s \tag{2b}$$

will also be of interest.

The derivative $S(r,r_c)$ has a definite geometrical meaning: it is the area of the cylindrical surface intersected by the sphere.

We will write down here the expressions for the quotients S/r and DA/r, rather than for S and DA,

$$\mathrm{Sr}(r,r_c)=\frac{1}{r}\partial V(r,r_c)/\partial r, \tag{3a}$$

$$\mathrm{DAr}(r,r_c)=\frac{1}{r}\partial A(r,r_c)/\partial r. \tag{3b}$$

Any of the six functions just defined, V, A, Vt, At, Sr and DAr, can be expressed in terms of elliptic integrals when r, r_c and R_p are such that effectively there is intersection between the sphere and the cylindrical surface, $|r_c-r|\leqslant R_p$.

Elliptic integrals should be reduced to standard forms for computation purposes. Although Legendre's standard elliptic integrals of first, second and third types have been customarily used to reduce elliptic integrals, Carlson has given alternative definitions of standard elliptic integrals, which allow the use of efficient computational codes (see e.g. Press, Teukolsky, Vetterling, & Flannery, 1992). Some other advantages of Carlson's definitions can be appreciated in the bibliography quoted in Press et al. (1992). Carlson's standard elliptic integrals are defined below

First kind:

$$R_F(x,y,z)=\frac{1}{2}\int_0^{\infty}\frac{\mathrm{d}t}{\sqrt{(t+x)(t+y)(t+z)}}, \tag{4a}$$

where x, y, z should be non-negative and at most one can be zero.

Second kind:

$$R_D(x,y,z)=\frac{3}{2}\int_0^{\infty}\frac{\mathrm{d}t}{(t+z)\sqrt{(t+x)(t+y)(t+z)}}, \tag{4b}$$

where x, y should be non-negative and at most one can be zero; z must be positive.

Third kind:

$$R_J(x,y,z,p)=\frac{3}{2}\int_0^{\infty}\frac{\mathrm{d}t}{(t+p)\sqrt{(t+x)(t+y)(t+z)}}, \tag{4c}$$

where x, y, z should be non-negative and at most one can be zero; p must be non-zero (if p is negative the result is the Cauchy principal value).

Codes to evaluate Carlson's standard elliptic integrals are available in most software libraries. The Fortran double precision algorithms given by Press et al. (1992) were employed here for computation of the three types of integrals.

Following the procedure outlined in Appendix A, the six geometrical quantities can be expressed by

$$V(r,r_c)=\tfrac{4}{3}R_p^3[E_V(r,r_c)+\theta(r,r_c)], \tag{5a}$$

$$A(r,r_c)=4R_p^2[E_A(r,r_c)+\theta(r,r_c)], \tag{5b}$$

where

$$\theta(r,r_c)=\begin{cases}\pi & \text{if } r_c<r,\\ \pi/2 & \text{if } r_c=r,\\ 0 & \text{if } r_c>r.\end{cases} \tag{6}$$

For Vt and At,

$$\mathrm{Vt}(r,r_c)=\tfrac{4}{3}R_p^5[E_{\mathrm{Vt}}(r,r_c)+\Gamma(r,r_c)], \tag{7a}$$

$$\mathrm{At}(r,r_c)=4R_p^4[E_{\mathrm{At}}(r,r_c)+\Gamma(r,r_c)], \tag{7b}$$

where

$$\Gamma(r,r_c)=\frac{\pi}{R_p^2}\min(r^2,r_c^2). \tag{8}$$

For Sr and DAr,

$$\mathrm{Sr}(r,r_c)=8R_pE_S(r,r_c), \tag{9a}$$

$$\mathrm{DAr}(r,r_c)=8E_{\mathrm{DA}}(r,r_c). \tag{9b}$$

The terms $E(r,r_c)$ in Eqs. (5), (7) and (9) introduce the elliptic integrals, as detailed in Table 1, when there is intersection between the sphere and the cylindrical surface, $|r_c-r|\leqslant R_p$. If not, they should be taken as zero when using Eqs. (5), (7) and (9). There are some combinations of r and r_c values for which some terms in Table 1 become undetermined, as explained in Appendix B. In practice, to cover all possible values of r and r_c, Table 2 includes the particular cases for which the formulation in Table 1 either should not be used or may be avoided.

Case 1 in Table 2 is the trivial case without intersection, $|r_c-r|>R_p$. Case 2 is defined when $r=r_c=0$.

Case 3 takes place strictly when $(r_c+r)=R_p$, but in practice it should be assumed when $k^2<10^{-25}$ (see the definition of k^2 in Table 1).

The occurrence of Cases 1–3 should be checked sequentially. Only if none of them is applicable, the expressions in Table 1 are to be used, taking the caution of assuming simultaneously $\mathscr{Z}_J=0$ and $\theta(r,r_c)=\pi/2$ (in Eqs. (5)) when $p<10^{-25}$ (see the definition of p in Table 1).

To our knowledge, the only expression previously employed in the context of particle distribution in fixed beds is $\mathrm{Sr}(r,r_c)$ (Mariani et al., 1998; Mariani, Mazza, Martínez, & Barreto, 2000). From Table 1, the expression of $\mathrm{Sr}(r,r_c)$ in the general case is

$$\mathrm{Sr}(r,r_c)=\frac{8R_p}{(\phi_M-\phi_B)^{1/2}}\times\left[(1-\phi_B)\mathscr{F}(k^2)-\frac{1}{3}(\phi_A-\phi_B)\mathscr{D}(k^2)\right]. \tag{9c}$$

It is also worth writing down the expression of DAr in the general case

$$\mathrm{DAr}(r,r_c)=\frac{8}{(\phi_M-\phi_B)^{1/2}}\mathscr{F}(k^2). \tag{9d}$$

From Eqs. (9c) and (9d) and the definition of k^2 in Table 1 it is easy to check that Sr and DAr are symmetrical functions under permutation of the arguments. Then, $\mathrm{Sr}(r,r_c)=\mathrm{Sr}(r_c,r)$ and $\mathrm{DAr}(r,r_c)=\mathrm{DAr}(r_c,r)$. This property will be employed in the following sections.

3. Voidage profiles expressed from the particle center distribution

Since voidage is primarily defined as a volumetric property, we start defining the average local voidage on an annular cylinder defined by radii r and $r+\Delta r$. Then, $\bar{\varepsilon}(r,\Delta r)$ is defined as the fraction of voids in that volume, and can be expressed as $\bar{\varepsilon}(r,\Delta r)=1-\bar{v}_p(r,\Delta r)$, where $\bar{v}_p(r,\Delta r)$ is the volumetric fraction of particles.

The distribution of particle centers is defined by the number density function $\rho(r_c)$, such that $[2\pi\rho(r_c)r_c\,\mathrm{d}r_c]$ is the number of particle centers per unit bed length between r_c and $r_c+\mathrm{d}r_c$. Then, $\bar{v}_p(r,\Delta r)$ can be expressed by

$$\begin{aligned}1-\bar{\varepsilon}(r,\Delta r)&=\bar{v}_p(r,\Delta r)\\&=\frac{2\pi\int_0^R[V(r+\Delta r,r_c)-V(r,r_c)]\rho(r_c)r_c\,\mathrm{d}r_c}{\pi[(r+\Delta r)^2-r^2]},\end{aligned} \tag{10a}$$

where R is the tube radius.

In particular, the average bed voidage $\bar{\varepsilon}$ can be expressed from Eq. (10a) as $\bar{\varepsilon}=\bar{\varepsilon}(0,R)$. Then, as $V(R,r_c)=\frac{4}{3}\pi R_p^3$, $V(0,r_c)=0$, $\bar{\varepsilon}=1-\frac{8}{3}\pi R_p^3\int_0^R\rho(r_c)r_c\,\mathrm{d}r_c/R^2$.

Although $\bar{\varepsilon}(r,\Delta r)$ is conceptually helpful and it should be employed for analyzing experimental data or in the frame of zone models for packed beds (Legawiec & Ziólkowski, 1994), a continuous description is frequently employed. For this, it is clear that a local radial voidage defined as $\varepsilon(r)=\lim_{\Delta r\to 0}\bar{\varepsilon}(r,\Delta r)$ allows a neat description of the local voidage profile. The corresponding local volumetric fraction of solid $v_p(r)$ can be readily calculated from Eq. (10a) by applying the L'hopital rule and

Table 1
Expressions for functions $E(r, r_c)$ in the general case defined by $|r_c - r| \leqslant R_p$, but excluding $r = r_c = 0$ and $(r + r_c) = R_p$

Define: $\phi_B = [(r_c - r)/R_p]^2$, $\phi_S = [(r_c + r)/R_p]^2$, $\phi_A = \min(1, \phi_S)$, $\phi_M = \max(1, \phi_S)$,
and consider the elliptic integrals

$$\mathscr{F} = R_F(0, k^2, 1);\ \mathscr{D} = R_D(0, k^2, 1);\ \mathscr{J} = R_J(0, k^2, 1, p)$$

where $k^2 = (\phi_M - \phi_A)/(\phi_M - \phi_B)$ and $p = (\phi_B/\phi_A)k^2$. Then,

$$E = \frac{1}{(\phi_M - \phi_B)^{1/2}}\left[\left(\alpha + \beta\phi_B + \frac{\gamma}{\phi_A}\right)\mathscr{F} + \frac{1}{3}(\phi_A - \phi_B)(\mathscr{Z}_J + \beta\mathscr{D})\right], \tag{T1}$$

where

$$\mathscr{Z}_J = \begin{cases} (\gamma/\phi_A^2)k^2\mathscr{J} & \text{when } \gamma \neq 0 \\ 0 & \text{when } \gamma = 0 \end{cases}$$

and

	α	β	γ
E_S	1	-1	0
E_{DA}	1	0	0
E_V	$\frac{1}{3}(\sigma + \Delta^2 - 6\Delta - 3)$	$\frac{1}{3}(4 + 3\Delta - 2\sigma)$	Δ
E_A	$-(1 + \Delta)$	1	Δ
E_{Vt}	$\frac{1}{15}(\sigma^2 + \sigma\Delta^2 - 9\sigma - 18\Delta^2)$	$\frac{1}{15}(3 - 2\sigma^2 + 7\sigma + 6\Delta^2)$	Δ^2
E_{At}	$-\frac{2}{3}(\sigma + \Delta^2)$	$\frac{1}{3}(1 + \sigma)$	Δ^2
	$\Delta = (r_c^2 - r^2)/R_p^2$,	$\sigma = 2(r_c^2 + r^2)/R_p^2$	

Table 2
Particular cases for the evaluation of functions $E(r, r_c)$

	$\lvert r_c - r\rvert > R_p$ Case 1	$r_c = r = 0$ Case 2	$(r + r_c) = R_p$ Case 3
E_S	0	$\pi/2$	$\frac{2}{R_p}(rr_c)^{1/2}$
E_{DA}	0	$\pi/2$	∞
$(E_V + \theta)$	θ	0	$\arccos\left(\frac{r_c - r}{R_p}\right) - \frac{2}{R_p^3}(r_c r)^{1/2}\left(\frac{8}{3}r_c r + r_c^2 - r^2\right)$
$(E_A + \theta)$	θ	0	$\arccos\left(\frac{r_c - r}{R_p}\right) - \frac{2}{R_p}(r_c r)^{1/2}$
$(E_{\mathrm{Vt}} + \Gamma)$	Γ	0	$\vartheta + \frac{2}{R_p^5}(r_c r)^{1/2}\left(\frac{24}{5}(r_c r)^2 + \frac{4}{3}r_c r(r_c^2 + r^2) - R_p^4\right)$
$(E_{\mathrm{At}} + \Gamma)$	Γ	0	$\vartheta + \frac{2}{R_p^3}(r_c r)^{1/2}\left(\frac{4}{3}r_c r - R_p^2\right)$

$$\theta = \begin{cases} \pi & \text{if } r_c < r, \\ \pi/2 & \text{if } r_c = r, \\ 0 & \text{if } r_c > r. \end{cases} \qquad \Gamma = \frac{\pi}{R_p^2}\min(r^2, r_c^2), \qquad \vartheta = \pi\left(\frac{r}{R_p}\right)^2 + \frac{r_c - r}{R_p}\arccos\left(\frac{r_c - r}{R_p}\right)$$

Eqs. (1a) and (3a):

$$1-\varepsilon(r)=v_p(r)=\frac{\int_0^R [\mathrm{d}V(r,r_c)/\mathrm{d}r]\rho(r_c)r_c\,\mathrm{d}r_c}{r}=\int_0^R \mathrm{Sr}(r,r_c)\rho(r_c)r_c\,\mathrm{d}r_c. \tag{10b}$$

Since at constant r_c we can express from Eq. (1a) $[V(r+\Delta r,r_c)-V(r,r_c)]=\int_r^{r+\Delta r} S(r,r_c)\,\mathrm{d}r$, a direct relationship between $\varepsilon(r)$ and $\bar{\varepsilon}(r,\Delta r)$ can be written from Eqs. (10a) and (10b) as

$$\bar{\varepsilon}(r,\Delta r)=\frac{2}{\Delta r(2r+\Delta r)}\int_r^{r+\Delta r}\varepsilon(r)r\,\mathrm{d}r. \tag{10c}$$

If we recall that in randomly packed beds particles are accommodated from the vessel wall as a series of layers with a decreasing degree of order, the density function $\rho(r_c)$ can be conceived as built up from the contributions of a series of zones of high concentration of particle centers separated by spaces of negligible particle concentration. The first zone, corresponding to particles with centers tightly close to a distance $y=R_p$ from the wall, will show the highest density of particle centers and a very thin width. The second zone will be confined about $y=3R_p$, but it will be thicker and will show lower particle center density than the first one. This trend is maintained toward the interior of the bed and, if the aspect ratio $a=R/R_p$ is high enough, a point is reached from which the zones overlap (i.e. no spaces are left in between), defining an innermost fully randomized region which extends up to the bed axis. This region can be considered as a last zone with uniform density of particle centers. From this description, it is better to write down $\rho(r_c)$ as the sum of the zone contributions rather than as a continuous function,

$$\rho(r_c)=\sum_{j=1}^{M}\rho_j(r_c). \tag{11a}$$

From Eq. (10b),

$$1-\varepsilon(r)=v_p(r)=\sum_{j=1}^{M}P_j(r), \tag{11b}$$

where $P_j(r)$ is the contribution of zone j,

$$P_j(r)=\int_0^R \mathrm{Sr}(r,r_c)\rho_j(r_c)r_c\,\mathrm{d}r_c. \tag{11c}$$

For the average voidage $\bar{\varepsilon}(r,\Delta r)$ (Eq. (10a)),

$$1-\bar{\varepsilon}(r,\Delta r)=\bar{v}_p(r,\Delta r)=\frac{1}{\Delta r(2r+\Delta r)}\sum_{j=1}^{M}\bar{P}_j(r,\Delta r), \tag{11d}$$

where $\bar{P}_j(r,\Delta r)$ is the contribution of the jth zone.

$$\bar{P}_j(r,\Delta r)=2\int_0^R \Delta V(r,\Delta r,r_c)\rho_j(r_c)r_c\,\mathrm{d}r_c, \tag{11e}$$

with

$$\Delta V(r,\Delta r,r_c)=V(r+\Delta r,r_c)-V(r,r_c). \tag{11f}$$

As it will be discussed below, essentially in all references found in bibliography the zones have been defined as containing particle centers ideally concentrated at one position or uniformly distributed. Mathematically, an impulse function represents the first case and a step function the second one. Expressions (11c) and (11e) will be next applied for either case.

For an impulse function acting at radius r_j,

$$\rho_j(r_c)=N_j\delta(r_c,r_j), \tag{12a}$$

where N_j is the number of particles in the jth zone per unit bed length, and the impulse function is normalized according to $2\pi\int_0^R \delta(r_c,r_j)r_c\,\mathrm{d}r_c=1$.

Eq. (11c) becomes

$$P_j(r)=\frac{1}{2\pi}N_j\mathrm{Sr}(r,r_j). \tag{12b}$$

From Eqs. (11e) and (11f),

$$\bar{P}_j(r,\Delta r)=\frac{1}{\pi}N_j[V(r+\Delta r,r_j)-V(r,r_j)]. \tag{12c}$$

For a zone with particle centers distributed as a step function in the interval $[r_j^i,r_j^e]$,

$$\rho_j(r_c)=\left\{\begin{array}{ll}\bar{\rho}_j & \text{if } r_c\in[r_j^i,r_j^e]\\ 0 & \text{if } r_c\notin[r_j^i,r_j^e]\end{array}\right\},$$

$$\bar{\rho}_j=\frac{N_j}{\pi[(r_j^i)^2-(r_j^e)^2]}. \tag{13a}$$

According to Eq. (11c),

$$P_j(r)=\bar{\rho}_j\int_{r_j^i}^{r_j^e}\mathrm{Sr}(r,r_c)r_c\,\mathrm{d}r_c. \tag{13b}$$

We recall that $\mathrm{Sr}(r,r_c)$ is a symmetrical function under permutation of the arguments r and r_c. Then, $\mathrm{Sr}(r,r_c)=\mathrm{Sr}(r_c,r)=S(r_c,r)/r_c$. Therefore, we can replace in Eq. (13b) $\mathrm{Sr}(r,r_c)r_c=S(r_c,r)$. Besides, at constant r, $S(r_c,r)\,\mathrm{d}r_c=\mathrm{d}V(r_c,r)$. Then, Eq. (13b) becomes

$$P_j(r)=\bar{\rho}_j[V(r_j^e,r)-V(r_j^i,r)]. \tag{13c}$$

Noting the order of the arguments of V in Eq. (13c), the term in the square brackets is the volume of a particle centered at a distance r from the bed axis intersected by the annular cylinder between the radii r_j^i and r_j^e.

From Eq. (11e),

$$\bar{P}_j(r,\Delta r)=2\bar{\rho}_j\int_{r_j^i}^{r_j^e}\Delta V(r,\Delta r,r_c)r_c\,\mathrm{d}r_c. \tag{13d}$$

Accounting for Eq. (11f) and the definition of $\mathrm{Vt}(r,r_c)$, Eq. (2a),

$$\bar{P}_j(r,\Delta r)=\bar{\rho}_j[\mathrm{Vt}(r+\Delta r,r_j^e)-\mathrm{Vt}(r+\Delta r,r_j^i)+\mathrm{Vt}(r,r_j^i)-\mathrm{Vt}(r,r_j^e)]. \tag{13e}$$

Eqs. (11)–(13) allow to evaluate $\varepsilon(r)$ and $\bar{\varepsilon}(r,\Delta r)$ without numerical integration, if the geometrical quantities defined in Eqs. (5)–(9) and Tables 1, 2 are employed.

As regards Eq. (13e), when both $r, r_c \gg R_p$, it is convenient for avoiding truncation losses to perform the operation between the square brackets for the four terms Γ (Eq. (8)) on one side, and for the terms E_{Vt} on the other, as the individual values of Γ may become very large, while their difference may not.

The contributions P_j or $\bar{P}_j$ will be zero if particles in the jth zone do not intersect the radius r or the annulus between r and $(r+\Delta r)$. Hence, the summation in Eqs. (11b) or (11d) may extend over a limited number of zones. The zones effectively contributing can be either identified beforehand or, if the geometrical quantities are defined as in Tables 1 and 2, the value of V, Sr or Vt will directly discriminate whether there is intersection or not.

The works in bibliography dealing with the relationship between voidage profile and particle center distribution have different aims and scopes. Some of them will be briefly commented on next to show how Eqs. (11)–(13) can be used in practice and how expressions given in the previous section for $\mathrm{Sr}(r,r_c)$, $\mathrm{V}(r,r_c)$ and $\mathrm{Vt}(r,r_c)$ facilitate going back and forth between voidage profile and particle center distribution, without resorting to geometrical simplifications or numerical integration.

Ridgway and Tarbuck (1968) proposed to evaluate $\varepsilon(r)$ by considering a series of perfectly ordered layers of particles with variable spacing between them that depends on the bed aspect ratio. It follows that their expression would correspond to Eq. (11b) with all the zones defined by impulse functions Eq. (12a). Each contribution P_j would be given by Eq. (12b), which can be written as

$$P_j(r) = \frac{1}{2\pi} N_j \left[\frac{S(r,r_j)}{r}\right]. \tag{14a}$$

Instead, they are expressed as

$$P_j(r) = n_j S_{II}(r_j - r) = \frac{1}{2\pi} N_j \left[\frac{S_{II}(r_j - r)}{r_j}\right], \tag{14b}$$

where $n_j = N_j/(2\pi r_j)$ is the number of particles per unit area of the surface containing the particle centers, and $S_{II}(r_j - r) = \pi[R_p^2 - (r_j - r)^2]$ is the area resulting from the intersection of a particle centered at r_j and a plane normal to the radius r_j at a position r. Actually, the proposed expression was derived from the case of a bed confined by a flat wall, a case in which Eq. (14b) is completely correct. When aimed to cylindrical vessels, we can appreciate by comparing Eqs. (14a) and (14b) that two approximations are involved: the use of S_{II} instead of S (neglecting the curvature effect in the intersected area S) and the radius r_j replacing r. These approximations will become noticeable for relatively low aspect ratios. Nonetheless, Ridgway and Tarbuck (1968) did not test the expression for aspect ratios less than $a = 17.3$.

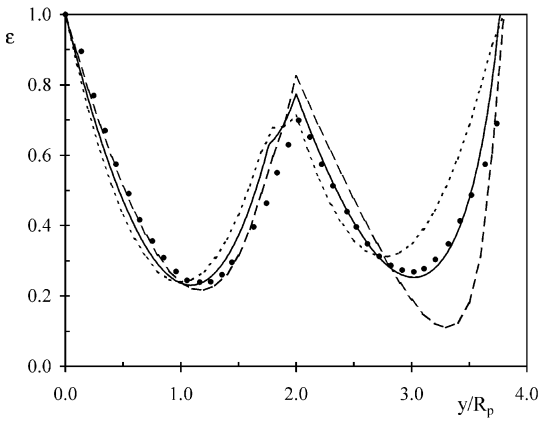

Fig. 1. Radial voidage profile at $a = 3.96$. (•) Experimental data points (Mueller, 1992); (——) values from Eq. (14a); (- - - - -) values from Eq. (14b); (– – – –) values from Eq. (14c).

Kubie (1988) proposed a similar model, also expressed by Eq. (14b), but limited to the first two layers. Therefore, the voidage can be evaluated up to distances from the wall not much longer than $y = 3R_p$.

According to the concepts discussed above, the second zone will already present an appreciable dispersion of particle centers, rather than exhibiting a sharp concentration of particle centers, as assumed by Kubie (1988) or Ridgway and Tarbuck (1968).

Nonetheless, it is interesting to mention that for some specific aspect ratios a two zone model with concentrated particle centers, just as in Kubie's approach, provides a good description for particle distribution. In Fig. 1, the local voidage profile $\varepsilon(r)$ reported by Mueller (1992) (a comment about his experimental technique is given below) for an aspect ratio $a = 3.96$ is presented. The results by considering two layers concentrated at $r_1 = R - R_p$ with $(N_1 R_p) = 4.50$, and $r_2 = (R - 2.764R_p)$ with $(N_2 R_p) = 1.65$, are also displayed in Fig. 1. Three formulations are considered: Eqs. (14a), (14b), and

$$P_j(r) = \frac{1}{2\pi} N_j \left[\frac{S_{II}(r_j - r)}{r}\right]. \tag{14c}$$

Eq. (14c) corrects Eq. (14b) as regards the ratio (r_j/r), but leaves S_{II} in place of S.

Expression (14a) produces a good approximation for essentially the whole bed section. The reason why in this case a second zone defined by an impulse function provides a good match with the experimental data can be ascribed to the fact that the tube size just allows the accommodation of four particles along its diameter.

Fig. 1 also permits to evaluate the deviations from Eqs. (14b) and (14c). Up to distances from the wall of about $y = R_p$, the maximum relative deviations between Eqs. (14a) and (14b) and also between Eqs. (14a) and (14c) rise up to about 10%. The differences grow towards

the bed axis, and it can be appreciated in Fig. 1 that Eqs. (14b) and (14c) become unsound in the last part of the profile.

Considering now higher aspect ratios than that in Fig. 1, it is worth noting that the Ridgway and Tarbuck (1968) expression predicts waves in the $\varepsilon(r)$ profile showing two small cusps close to each other instead of a single maximum (as insinuated in Fig. 1 in the region close to $y=2R_p$), a feature not found in experimental profiles. This effect is due to the assumption of sharply concentrated particle centers in the second and following zones.

To our knowledge, the first work in which the general relationship between the distribution of particle centers and the local voidage profile has been formally stated was the monograph of Singleton (1971). His expression (written with the present nomenclature) can be written from Eq. (10b) by recalling the already used equivalence $\mathrm{Sr}(r,r_c)r_c=S(r_c,r)$:

$$1-\varepsilon(r)=\int_0^R \rho(r_c)S(r_c,r)\,\mathrm{d}r_c=\int_0^R \rho(r_c)\,\mathrm{d}V(r_c,r).$$

Singleton employed this expression to evaluate $\rho(r_c)$ from voidage profile data presented by Benenatti and Brosilov (1962). He considered a first zone with particle centers concentrated at $y=R_p$ (Eq. (12a)) and a series of concentric rings in which ρ_j are defined as step functions (Eq. (13a)). To evaluate the contributions P_j, he used an approximation which can be expressed as $S(r_c,r)\approx(r_c+r)S_{II}(r_c-r)/(2r)$, from which analytical expressions arise for P_j when $\rho_j(r_c)$ is defined either by Eq. (12a) or by Eq. (13a). Singleton adjusted the values of N_j for the impulse function and for two alternative sets of rings, one with 29 rings extending up to about $y=7R_p$ and the other with 21 rings up to about $y=4R_p$. In some rings values $N_j\approx 0$ were found. Expressions to evaluate the effect of the aspect ratio a (from $a\to\infty$ down to $a=5.6$) on the positions of the rings and on N_j were also presented. More comments on Singleton's work will be made in the next section.

Govindarao and Froment (1986) performed a work similar to that of Singleton (1971), considering rings of uniform width, typically $\Delta r=R_p/3$ or $R_p/4$. Within each ring, the concentration of particle centers was also assumed to be uniform (Eq. (13a)), including the ring closest to the wall, $r_1^e=R-R_p$. Govindarao and Froment (1986) provided an expression to evaluate the average voidage within each ring, $\bar{\varepsilon}(r_k^i,\Delta r)$, with $r_k^i=R-(R_p+k\Delta r)$. Their expression can be interpreted from Eq. (11e) for the contribution of particle centers from the ring j to the ring k,

$$\bar{P}_j(r_k^i,\Delta r)=2\,\bar{\rho}_j\int_{r_j^i}^{r_j^i+\Delta r}\Delta V(r_k^i,\Delta r,r_c)r_c\,\mathrm{d}r_c. \qquad (15a)$$

The effect of the curvature was then ignored in two senses. The radius r_c is removed from the integrand and evaluated as the average value in the jth ring, $r_j^i+\frac{1}{2}\Delta r$, and $\Delta V(r_k^i,\Delta r,r_c)$ is approximated by $\Delta V_{II}(r_k^i-r_c,r_k^i+\Delta r-r_c)$, the volume of a particle centered at r_c intersected between two planes normal to radius r_c at positions r_k^i and $r_k^i+\Delta r$. With these assumptions and expressing $\bar{\rho}_j$ from Eq. (13a), Eq. (15a) can be written as

$$\bar{P}_j(r_k^i,\Delta r)=\frac{N_j}{\Delta r}\int_{r_j^i}^{r_j^i+\Delta r}\Delta V_{II}(r_k^i-r_c,\ r_k^i+\Delta r-r_c)\,\mathrm{d}r_c. \qquad (15b)$$

As ΔV_{II} is defined by an elementary expression, the integration in Eq. (15b) can be performed analytically.

Once the result of Eq. (15b) is replaced in Eq. (11d), the final expression for $\bar{\varepsilon}(r_k^i,\Delta r)$ used by Govindarao and Froment (1986) can be obtained. They employed this expression to assess N_j from experimental values of $\bar{\varepsilon}(r_k^i,\Delta r)$, choosing Δr according to the values employed in the experimental evaluations. From the wall up to distances $y\approx 4R_p$ only the first ring ($R_p<y<R_p+\Delta r$) and that between $3R_p-\Delta r<y<3R_p$ were found to contain a significant number of particles, in agreement with the presence of the first two particle layers. Deeper inside the bed, up to around $8R_p$, some rings were also found to be almost empty and others showed a significant amount of particles. They identified nine filled rings up to $y=8R_p$.

The results from the work of Govindarao and Froment (1986) were reanalyzed afterwards, but considering only the first two filled rings (Govindarao & Ramrao, 1988), or the first four filled rings (Delmas & Froment, 1988).

More recently, Mariani et al. (1998), following a similar line to that in the work of Govindarao and Froment (1986), presented a model with only two zones of finite width intending to identify just the first two particle layers closest to the wall. The remaining particles in the bed were assumed to be in a third zone with uniform density of particle centers. Instead of assuming uniform ρ_j in the first two zones, they tried shape factors $f_j(r_c)$, such that $\rho_j(r_c)=\bar{\rho}_j f_j(r_c)$, $j=1,2$. For the second zone, no better results than those for a step function ($f_2=1$) were obtained. Instead, the first zone was better modelled by taking f_1 as a linear function in r_c, with the maximum value at $r_1^e=R-R_p$ and zero at $r_1^i=R-1.2R_p$. The relatively thin width of the first zone ($\Delta r_1=R_p/5$ as compared, for example, with $R_p/3$ employed by Delmas and Froment, 1988) and the shape factor $f_1(r_c)$ were needed to get a good fit of the steep drop of local voidage close to the wall, a feature clearly found in most experimental data sets.

Mariani et al. (1998) worked with local values $\varepsilon(r)$, as expressed by Eq. (11b). They used the function $\mathrm{Sr}(r,r_c)$

as given here (Eq. (9c) for the general case), and numerically integrated Eq. (11c) to obtain P_j for their three zones. It is interesting to remark that for $f_j = a + br_c$ (i.e. for their first zone) there is apparently no way to express P_j analytically or as an elliptic integral. Instead, if f_j is defined by a polynomial in r_c^2 (the simplest one being $f_j = a^* + b^* r_c^2$), P_j can be expressed in terms of elliptic integrals through an expression like (T1) in Table 1. However, we will not pursue here an extension in this direction, as the best way to deal with the first zone seems to be the use of an impulse function (Eq. (10a)), while the remaining zones can be well modelled by simple step functions. This is actually the approach followed by Singleton (1971).

Mueller (1992,1999), by employing an X-ray technique, measured the position of every particle in vertical segments of his experimental beds. From these measurements, Mueller reported voidage profiles, in terms of $\bar{\varepsilon}(r, \Delta r)$. His evaluations can be described by means of Eqs. (11d) and (12c), if M refers to the total number of observed particles and N_j in Eq. (12c) is taken as the inverse of the length of the analyzed bed segment (each observed particle is associated to an impulse function at its radial position). Mueller (1992,1999) evaluated $V(r, r_c)$ in Eq. (12c) by numerical integration, (from a geometrical formulation similar to that given in Appendix A). The reported profiles of $\bar{\varepsilon}(r, \Delta r)$ were obtained by diminishing Δr up to a point below which the results did not appreciably change. Actually, these calculations correspond to the local voidage $\varepsilon(r)$ for which Eqs. (11b) and (12b) apply.

Mueller's works were aimed at developing empirical expressions to predict voidage profiles, rather than characterizing the distribution of particle centers.

Legawiec and Ziólkowski (1994) measured the position and number of particles in the first layer adjacent to the wall. They proved that essentially all particles are in contact with the wall. They did not evaluate the position of particles already belonging to the second layer (centered at a distance around $3R_p$ from the wall), but found that a certain number of particles remain centered at a distance around $2R_p$ from the wall. These particles can stay in that position by taking advantage of holes (defects in the two-dimensional particle array) in the first layer. Nonetheless, the number of these particles were relatively low: about 2% of the number of particles contacting the wall were centered between $1.8R_p < y < 2R_p$ and 10% between $2R_p < y < 2.2R_p$. The main purpose of their measurements was to evaluate the average voidage from the wall up to a distance $y = R_p$, i.e. $\bar{\varepsilon}(R - R_p, R_p)$, for its use in their model of conductivity within the near-wall region. To this end, and according to the previous description, only the particles contacting the wall (i.e. with centers concentrated at $R - R_p$) should be considered in practice. In expressing $\bar{\varepsilon}(R - R_p, R_p)$, they employed an equation like Eq. (11d) with $M = 1$ for $\bar{\varepsilon}(R - R_p, R_p)$ and Eq. (12c) for $\bar{P}_1(R - R_p, R_p)$:

$$\bar{P}_1(R - R_p, R_p) = \frac{1}{\pi} N_1 [V(R, R - R_p) - V(R - R_p, R - R_p)]. \quad (16)$$

$V(R, R - R_p) = \frac{4}{3}\pi R_p^3$ and $V(R - R_p, R - R_p)$ was evaluated by Legawiec and Ziólkowski (1994) numerically, in a similar fashion as done by Mueller (1992,1999). It is illustrative to write down the expression resulting for $\bar{\varepsilon}(R - R_p, R_p)$ by using Eq. (5a) and Table 1 (the general case applies if $a \neq 1.5$) for $V(R - R_p, R - R_p)$. In Table 1, $r = r_c = R - R_p$. By using $a = R/R_p$,

$$(a \neq 1.5) \quad 1 - \bar{\varepsilon}(R - R_p, R_p) = N_1 R_p \frac{(4/3)}{\pi(2a - 1)} \left\{ \frac{\pi}{2} - \frac{1}{3\phi_M^{1/2}} [(\phi_S - 3)\mathscr{F} + \frac{2}{3}\phi_A(2 - \phi_S)\mathscr{D}] \right\}, \quad (17)$$

where $\phi_S = 4(a-1)^2$, $\phi_A = \min(1, \phi_S)$, $\phi_M = \max(1, \phi_S)$, $k^2 = (\phi_M - \phi_A)/\phi_S$, $\mathscr{F}(k^2)$, $\mathscr{D}(k^2)$ are defined in Table 1.

For $a = 1.5$, Case 3 in Table 2 applies. Then, $[1 - \bar{\varepsilon}(R - R_p, R_p)] = \frac{1}{3} N_1 R_p (1 + 4/(3\pi))$ is obtained.

Beds with aspect ratios in the range $1 < a \leqslant 2$ constitute a special case in which all particles are touching the tube wall and the number of particles per unit length (N_1) can be evaluated from geometrical concepts (Govindarao, Ramrao, & Rao, 1992). The radial voidage profiles are then expressed by Eqs. (11b) and (11d) with $M = 1$ and P_1, $\bar{P}_1$ given by Eqs. (12b) and (12c) with $r_1 = R - R_p$. Then,

$$1 - \varepsilon(r) = \frac{1}{2\pi} N_1 \mathrm{Sr}(r, R - R_p), \quad (18a)$$

$$1 - \bar{\varepsilon}(r, \Delta r) = \frac{N_1}{\pi \Delta r (2r + \Delta r)} [V(r + \Delta r, R - R_p) - V(r, R - R_p)]. \quad (18b)$$

Govindarao et al. (1992) analyzed the voidage profiles in terms of Eq. (18b) with V evaluated numerically. The quantity $\mathrm{Sr}(r, r_c)$, as expressed by Eq. (9c), was introduced by Mariani et al. (2000) to obtain a closed expression of $\varepsilon(r)$ (Eq. (18a)) for this range of aspect ratios.

4. Profiles of particle surface area expressed from the particle center distribution

Just as the volume fraction of particles varies according to the radial position, their external surface area per unit volume suffers similar variations.

We define the average density of particle surface area $\bar{a}_V(r, \Delta r)$ as the area of particle surfaces within an annular cylinder defined by radii r and $r + \Delta r$ per unit volume of the annular cylinder. The local density of particle surface area $a_V(r)$ is defined by the limit of $\bar{a}_V(r, \Delta r)$ as $\Delta r \to 0$.

To express $a_V(r)$ and $\bar{a}_V(r,\Delta r)$ in terms of the density of particle centers we employ directly Eq. (11a) for $\rho(r_c)$. Then, recalling the meaning of functions $A(r,r_c)$ and $\mathrm{DAr}(r,r_c)$, we find for

$$a_V(r)=\sum_{j=1}^{M} Q_j(r), \tag{19a}$$

where $Q_j(r)$ is the contribution of the jth zone, that

$$Q_j(r)=\int_0^R \mathrm{DAr}(r,r_c)\rho_j(r_c)r_c\,\mathrm{d}r_c. \tag{19b}$$

For

$$\bar{a}_V(r,\Delta r)=\frac{1}{\Delta r(2r+\Delta r)}\sum_{j=1}^{M}\bar{Q}_j(r,\Delta r), \tag{19c}$$

where $\bar{Q}_j(r,\Delta r)$ is the contribution of the jth zone,

$$\bar{Q}_j(r,\Delta r)=2\int_0^R \Delta A(r,\Delta r,r_c)\rho_j(r_c)r_c\,\mathrm{d}r_c, \tag{19d}$$

with

$$\Delta A(r,\Delta r,r_c)=A(r+\Delta r,r_c)-A(r,r_c). \tag{19e}$$

Considering either an impulse function or a step function for $\rho_j(r_c)$, and following a similar step to that for the voidage profiles, we obtain the following formulation.

For an impulse function acting at radius r_j,

$$Q_j(r)=\frac{1}{2\pi}N_j\mathrm{DAr}(r,r_j), \tag{20a}$$

$$\bar{Q}_j(r,\Delta r)=\frac{1}{\pi}N_j[A(r+\Delta r,r_j)-A(r,r_j)]. \tag{20b}$$

For a distributed zone with a step function in the interval $[r_j^i,r_j^e]$,

$$Q_j(r)=\bar{\rho}_j[A(r_j^e,r)-A(r_j^i,r)], \tag{21a}$$

$$\bar{Q}_j(r,\Delta r)=\bar{\rho}_j[\mathrm{At}(r+\Delta r,r_j^e)-\mathrm{At}(r+\Delta r,r_j^i)+\mathrm{At}(r,r_j^i)-\mathrm{At}(r,r_j^e)]. \tag{21b}$$

Eqs. (19)–(21) allow to evaluate $a_V(r)$ and $\bar{a}_V(r,\Delta r)$ without numerical integration, if the geometrical quantities defined in Eqs. (5)–(9) and Tables 1, 2 are employed.

A comment similar to that for Eq. (13e) can be made about Eq. (21b). When both $r,r_c \gg R_p$, we suggest performing the operation between the square brackets for the four terms Γ (Eq. (8)) on one side, and for the terms E_{At} on the other.

Singleton (1971), apparently for the first time, made use of the local density of particle surface area $a_V(r)$ and established its relationship with $\rho_j(r_c)$. In terms of the contribution $Q_j(r)$, he expressed

$$Q_j(r)=\int_0^R \mathrm{DA}(r_c,r)\,\rho_j(r_c)\,\mathrm{d}r_c$$

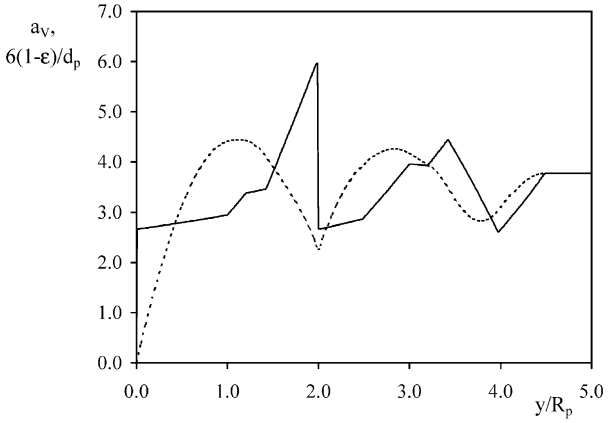

Fig. 2. Comparison of $a_V(r)$ (——) and $6[1-\varepsilon(r)]/d_p$ (- - - - - -) at $a=5.6$.

which is the same as Eq. (19b) by recalling the permutation property $\mathrm{DA}(r,r_c)/r=\mathrm{DA}(r_c,r)/r_c$.

Singleton (1971) evaluated numerically both $\mathrm{DA}(r_c,r)$ and the integral on r_c for his distribution model consisting of $\rho_1(r_c)$ given by an impulse function and $\rho_j(r_c)$, $j>1$ by step functions.

As mentioned in the previous section, Singleton could quantify the distribution of particle centers from voidage profiles, so he was able to evaluate $a_V(r)$. The purpose of Singleton calculations was to obtain profiles of the interstitial axial velocity, $u(r)$, which in turn he used to analyze mass dispersion experiments in packed beds.

In order to estimate $u(r)$, Singleton made use of the so-called Brinkman approach, which evaluates the local momentum transfer between fluid and particles by using Ergun, or any similar expression, written in terms of local properties. Specifically, Singleton used the Ergun expression

$$(\mathrm{d}p/\mathrm{d}z)_{fp}=-\frac{a_V(r)u(r)}{[\varepsilon(r)]^3}[4.17\mu_f a_V(r)+0.292\rho_f u(r)], \tag{22}$$

where $(\mathrm{d}p/\mathrm{d}z)_{fp}$ is the contribution of fluid–particle friction to pressure gradient.

In some works before that of Singleton, the term $a_V(r)$ in Eq. (22) was evaluated as $a_V(r)=6[1-\varepsilon(r)]/d_p$, which is the local version of $\bar{a}_V=\bar{a}_V(0,R)=6[1-\bar{\varepsilon}]/d_p$. While the latter relationship is true (as the overall bed quantities $\bar{a}_V$ and $\bar{\varepsilon}$ involve all the spheres in the beds), the former is not. Singleton pointed out this difference and used the values of $a_V(r)$ evaluated as described above in Eq. (22).

The difference between $a_V(r)$ and $6[1-\varepsilon(r)]/d_p$ can be appreciated in Fig. 2 for an aspect ratio $a=5.6$. The voidage profile data of Benenatti and Brosilov (1962) at this aspect ratio have been fitted to the following four-zone distribution of particle centers:

1st zone: impulse function at $r_1=R-R_p$; $(N_1 R_p)=6.75$,

2nd zone: step function between $r_2^i = R - 2.2R_p$ and $r_2^e = R - 2R_p$, $(N_2\ R_p) = 0.715$,

3rd zone: step function between $r_3^i = R - 2.97R_p$ and $r_3^e = R - 2.42R_p$; $(N_3\ R_p) = 3.63$,

4th zone: step function between $r_4^i = 0$ and $r_4^e = R - 3.49\ R_p$; $(N_4\ R_p) = 2.11$.

The definitions of the first and second zones were made according to the work of Legawiec and Ziólkowski (1994).

The differences shown in Fig. 2 are particularly noticeable in the regions $(0 < y < \frac{1}{2}R_p)$ and $(\frac{3}{2}R_p < y < 2R_p)$, where $a_V(r)$ is significantly larger than $6[1 - \varepsilon(r)]/d_p$. High local velocities $u(r)$ are predicted in these regions or zones, as a consequence of high values of $\varepsilon(r)$. The use of $a_V(r)$ instead of $6[1-\varepsilon(r)]/d_p$ (Eq. (22b)) reduces the magnitude of such high local velocities. Singleton (1971) mentioned that the permeability of the bed as arose from $u(r)$ profiles calculated with $6[1 - \varepsilon(r)]/d_p$ was (at low enough aspect ratios) significantly higher than that from experimental correlations. Instead, the use of $a_V(r)$ allowed him to obtain consistent results for $u(r)$.

In general, $a_V(r)$ or $\bar{a}_V(r, \Delta r)$ should be employed to evaluate the magnitude of any local transfer phenomena between the fluid phase and particles. Apart from the just discussed momentum transfer problem, heat and mass transfer between the fluid and particles are most important in packed beds applications. In spite of this, the distribution of particle surface area has seldom been considered since the work of Singleton, either in the literature concerning modelling of packed bed processes or in those works just dealing with packing properties.

For instance many models have been employed for multi-tubular catalytic reactors accounting for radial packing non-uniformities (e.g. Küfner & Hofmann, 1990; Papageorgiou & Froment, 1995; Cybulski, Eigenberger, & Stainkiewicz, 1997; Winterberg, Tsotsas, Krischke, & Vortmeyer, 2000). Essentially, in all of them composition and temperature differences between the local fluid flow and particles have been ignored, on account of the large superficial velocities typically employed in such reactors. This can explain the fact that the radial properties $a_V(r)$ or $\bar{a}_V(r, \Delta r)$ have not received attention in those works, as regards heat or mass transfer.

However, in most of those works profiles $u(r)$ calculated from Brinkman's approach were employed. In these and also in works specifically dealing with the evaluation of $u(r)$ (e.g. Bey & Eigenberger, 1997; Giese, Rottschäfer, & Vortmeyer, 1998; Subagyo, Standish, & Brooks, 1998), the use of $a_V(r)$ in Eq. (22) (or an equivalent) has been replaced by $6[1 - \varepsilon(r)]/d_p$.

It is worth stressing that $a_V(r)$ should be employed when composition or temperature differences between the local fluid flow and particles cannot be ignored, as typical operating conditions in multi-tubular catalytic reactors may not apply in all circumstances.

Finally, we mention here the work by Govindarao et al. (1992) concerning the structure of beds with aspect ratios in the range $1 < a \leqslant 2$, in which particle surface area profile has been evaluated. They referred to $\bar{a}_V\ (r, \Delta r)$, which from Eq. (19c) (with $M = 1$ and $r_1 = R - R_p$, as discussed in the previous section) and Eq. (20b) is expressed as

$$(1 < a \leqslant 2) \quad \bar{a}_V(r, \Delta r) = \frac{N_1}{\pi \Delta r(2r + \Delta r)}[A(r + \Delta r, R - R_p) - A(r, R - R_p)].$$

The values of A were calculated numerically in that work.

5. Conclusions

Expressions for geometrical quantities related to the intersection of a sphere and a cylindrical surface have been presented in terms of the natural functions arisen from integral calculus: elliptic integrals.

Four of these geometrical quantities, sphere volume (V) and surface (A) intersections and their derivatives (S and DA), are involved in the relations between radial profiles of voidage $[\varepsilon(r), \bar{\varepsilon}(r, \Delta r)]$ or specific particle surface area $[a_V(r), \bar{a}_V(r, \Delta r)]$ with the particle center distribution $[\rho(r)]$ in beds of uniform spheres.

The distribution of particle centers can be described by a series of zones presenting either concentrated or uniformly distributed particle centers. For this type of distributions, the four mentioned quantities plus the integrals of V and A (Vt and At) suffice to relate the radial profiles mentioned above with $\rho(r)$, without resorting to geometrical approximations or numerical integration.

Previous works allow to conclude that such type of distributions is suitable for practical purposes. In those contributions either geometrical approximations or numerical integration were always employed to relate radial voidage profiles with the distribution of particle centers.

The concept or definition of the density of particle surface area $[a_V(r), \bar{a}_V(r, \Delta r)]$ has been seldom invoked in bibliography, although it may be most relevant in evaluating radial velocity profiles and local heat and mass transfer rates between particles and fluid flow.

The identification of the density function of particle centers $\rho(r)$ for predictive purposes has received less attention than the development of voidage radial profiles. Nonetheless, $\rho(r)$ is a more basic information and it needs the identification of only a few zones. The knowledge of $\rho(r)$ allows not only the evaluation of voidage profiles, but also of particles surface area profiles and, intrinsically, of the number of particles in each layer. The last feature is essential when discrete models, accounting for the discontinuous nature of the solid phase, are employed. It is expected that the relations presented here, connecting the

profiles with $\rho(r)$ in a general way, may be helpful in shifting that trend. Although there is considerable knowledge about randomly packed, uniformly sized spheres, predictive expressions can still be improved. In addition, real spherical packings will usually present some dispersion in particle size. These cases are much less systematically studied, and further efforts are needed to obtain predictive expressions. The formulation presented here could be readily extended by assembling the contributions of particles in each size class.

Notation

A	area of a sphere surface left inside a cylindrical surface, m^2
At	integral defined in Eq. (2b), m^4
$\bar{a}_V(r,\Delta r)$	specific area of particle surfaces between radii r and $r+\Delta r$, m^{-1}
$a_V(r)$	specific area of particle surfaces at r, m^{-1}
a,	aspect ratio: R/R_p, dimensionless
DA	$\partial A/\partial r$, m
DAr	DA/r, dimensionless
d_p	particle diameter, m
N_j	number of particles in the jth zone per unit bed length, m^{-1}
R	internal tube radius, m
r	radial coordinate, m
R_p	sphere radius, m
r_c	radial position of a sphere center, m
S	area of a cylindrical surface intersected by a sphere, m^2
Sr	S/r, m
V	volume of a sphere left inside a cylindrical surface, m^3
Vt	integral defined in Eq. (2a), m^5
y	radial distance from the tube wall, m

Greek letters

$\bar{\varepsilon}(r,\Delta r)$	fraction of voids between radii r and $r+\Delta r$, dimensionless
$\varepsilon(r)$	voidage at r, dimensionless
$\rho(r_c)$	number density function of particle centers, m^{-3}
ρ_f	fluid density, kg m^{-3}
μ_f	fluid viscosity, kg s^{-1} m^{-1}

Acknowledgements

The authors wish to acknowledge the financial support of the following Argentine institutions:

ANPCyT-SECyT (PICT No. 00227), CONICET (PIP96 No. 4791), and UNLP (PID No. 11/I058). O.M.M. and G.F.B. are research members of the CONICET and N.J.M. is a fellow of the CONICET. The authors also thank an anonymous reviewer for providing the references Singleton (1971) and Dixon and Welch (1988).

Appendix A.

The procedure to develop the expressions of the geometrical quantities defined in Section 2 will be outlined here. The complete procedure can be requested from the authors.

To be specific, we will consider the evaluation of V and the other quantities will be briefly referred to later.

For non-trivial configurations ($r \neq 0$ and $|r_c - r| \leqslant R_p$), Fig. 3 corresponds to the cut of a plane (z,x), where z is the cylinder axis and the x-axis contains the sphere center. It can be visualized that V may be expressed from contributions of up to three geometrical bodies, depending on the values of r, r_c and R_p, $V = 2(V_{\text{cyl}} + V_{\text{cap}} + V_{\text{ell}})$. V_{cyl} is the volume of a cylinder of radius r and length z_A, which is only relevant for cases (b) and (d) in Fig. 3, where $z_A > 0$. V_{cap} is the volume of the spherical cap of height $(R_p - z_B)$, which should be included only when $r_c < r$, cases (a) and (b). Simple geometrical considerations lead to

$$z_A^2 = \max[0, R_p^2 - (r + r_c)^2], \qquad z_B^2 = R_p^2 - (r - r_c)^2 \tag{A.1}$$

from which V_{cyl} and V_{cap} can be elementarily calculated when it corresponds.

The third body presents an asymmetric shape and is found in all cases (Fig. 3). Its volume V_{ell} becomes expressed in terms of elliptic integrals, except for $R_p = (r + r_c)$ when the elliptic integrals degenerate into analytical expressions (expression in Table 2).

The evaluation of V_{ell} in the general case can be undertaken with the help of Fig. 4, where the cut of a transversal plane (y,x) at a generic position z, such that $z_A < z < z_B$, is depicted. From the coordinate axes defined in Figs. 3 and 4, it may be useful to take into account that the sphere surface is described by $(x - r_c)^2 + y^2 + z^2 = R_p^2$ and the cylinder surface by $x^2 + y^2 = r^2$. The circle of radius ρ in Fig. 4 corresponds to the intersection between the sphere and the plane (y,x). The relationship between ρ and z is

$$\rho^2 + z^2 = R_p^2. \tag{A.2}$$

From the areas of the sector O′PQ ($A_{\text{O′PQ}}$), the sector OPQ (A_{OPQ}) and the rhomb OPO′Q (A_{Rh}), the area of the lenticular surface QP (intersected surface) can be expressed as $(A_{\text{O′PQ}} + A_{\text{OPQ}} - A_{\text{Rh}})$. Then,

$$V_{\text{ell}} = \int_{z_A}^{z_B} (A_{\text{O′PQ}} + A_{\text{OPQ}} - A_{\text{Rh}})\, \mathrm{d}z, \tag{A.3}$$

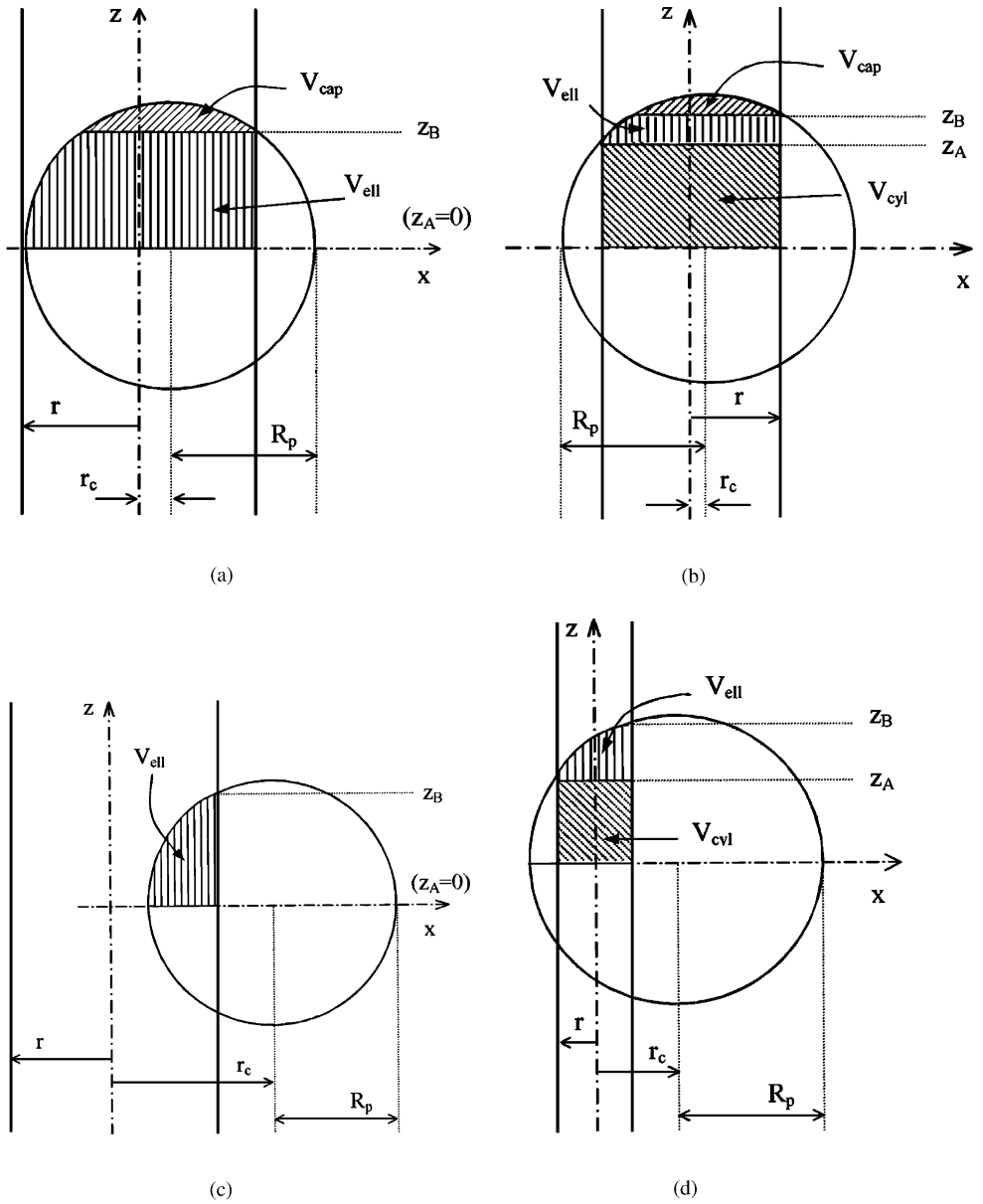

Fig. 3. Vertical cross section showing the intersection between a sphere of radius R_p and a cylindrical surface of radius r.

where (see Fig. 4)

$$A_{O'PQ} = \rho^2(\varphi') = \rho^2 \arccos\left(\frac{\rho^2 + r_c^2 - r^2}{2r_c\rho}\right),$$

$$A_{OPQ} = r^2(\varphi) = r^2 \arccos\left(\frac{\rho^2 + r_c^2 - r^2}{2r_c\rho}\right);$$

$$A_{Rh} = r_c y_I = r_c \left(\rho^2 - \frac{(\rho^2 + r_c^2 - r^2)^2}{4r_c^2}\right)^{1/2}. \qquad (A.4)$$

We will considered now the evaluation of $V_{O'PQ} = \int_{z_A}^{z_B} A_{O'PQ}\,dz$, which from Eqs. (A.2) and (A.4) can be expressed as

$$V_{O'PQ} = \int_{\rho_B}^{\rho_A} \rho^2 \arccos\left(\frac{\rho^2 + r_c^2 - r^2}{2r_c\rho}\right) \frac{\rho\,d\rho}{\sqrt{R_p^2 - \rho^2}}, \qquad (A.5)$$

where

$$\rho_A^2 = \min[r_p^2, (r + r_c)^2], \qquad \rho_B^2 = (r - r_c)^2.$$

Integrating Eq. (A.5) by parts with

$$u = \arccos\left(\frac{\rho^2 + r_c^2 - r^2}{2r_c\rho}\right), \qquad dv = \frac{\rho^3\,d\rho}{\sqrt{R_p^2 - \rho^2}}$$

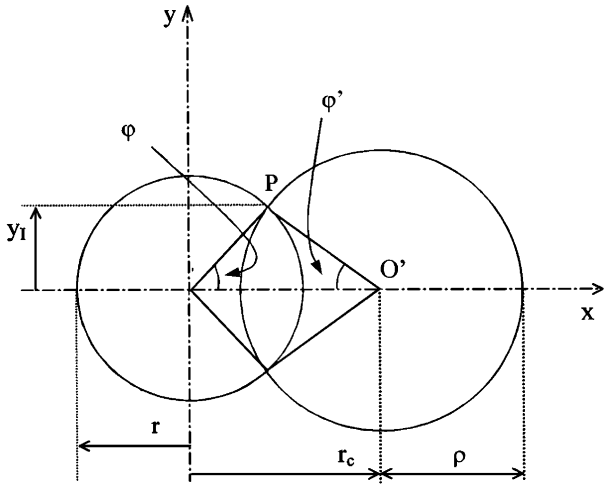

Fig. 4. Horizontal cross section showing the intersection between a sphere of radius R_p and a cylindrical surface of radius r.

and introducing $\phi=(\rho/R_p)^2$,

$$V_{\mathrm{O'PQ}}=(uv)|_{\rho_B}^{\rho_A}+\tfrac{1}{6}R_p^3 I, \tag{A.6}$$

with

$$\begin{aligned}(uv)|_{\rho_B}^{\rho_A}&=\tfrac{1}{3}R_p^3\left[-\arccos\left(\frac{\phi+\Delta}{2(r_c/R_p)\phi^{0.5}}\right)(\phi+2)(1-\phi)^{0.5}\right]_{\phi_B}^{\phi_A}\\&=\tfrac{1}{3}R_p^3\theta(\phi_B+2)(1-\phi_B)^{0.5},\end{aligned} \tag{A.7}$$

where $\phi_B=[(r_c-r)/R_p]^2$, $\phi_S=[(r_c+r)/R_p]^2$, $\phi_A=\min(1,\phi_S)$ (Table 1 in the main text), $\Delta=(r_c^2-r^2)/R_p^2$ and θ is defined in Eq. (6) given in the main text.

$$I=\int_{\phi_B}^{\phi_A}\mathscr{R}(\phi)\frac{\mathrm{d}\phi}{\sqrt{P(\phi)}}, \tag{A.8}$$

where

$$\mathscr{R}(\phi)=(\phi-\Delta)(\phi+2)(\phi-1)/\phi, \tag{A.9}$$

$$P(\phi)=(\phi-\phi_B)(\phi-\phi_S)(\phi-1). \tag{A.10}$$

Eq. (A.8) is an elliptic integral. By carrying out the division indicated by the rational function $\mathscr{R}(\phi)$, the result can be expressed in the form

$$\mathscr{R}(\phi)=a+b\phi+c/\phi+e\,\mathrm{d}P/\mathrm{d}\phi, \tag{A.11}$$

where $e=\frac{1}{3}$, $(-a)=2+[5\Delta+4(r/R_p)^2+\Delta^2]/3$, $b=[5+\Delta+8(r/R_p)^2]/3$, $c=2\Delta$.

$\mathscr{R}(\phi)$ can be expressed as in Eq. (A.11) because the integer part of the quotient and $\mathrm{d}P/\mathrm{d}\phi$ are both second-degree polynomials. Once $\mathscr{R}(\phi)$ from Eq. (A.11) is replaced in Eq. (A.8), we can appreciate that the resulting analytical term $(2e)\sqrt{P(\phi)}|_{\phi_B}^{\phi_A}=0$. Then,

$$I=\int_{\phi_B}^{\phi_A}(a+b\phi+c/\phi)\frac{\mathrm{d}\phi}{\sqrt{P(\phi)}}. \tag{A.12}$$

The terms in a,b,c are generic elliptic integrals of 1st, 2nd and 3rd kind, respectively. To convert these integrals into Carlson's standard elliptic integrals, we define first $\phi_M=\max(1,\phi_S)$, from which $P(\phi)=(\phi-\phi_B)(\phi-\phi_A)(\phi-\phi_M)$. This expression clearly reveals that the limits of integration are coincident with two roots of $P(\phi)$. When this happens, the integrals are called complete elliptic integrals. In general, it suffices that just one limit of integration be coincident with a root of $P(\phi)$ to facilitate the conversion into Carlson's standard elliptic integrals. The substitution $\phi=(t\phi_{L1}+\delta\phi_{L2})/(t+\delta)$, where t is the new variable, δ is any positive constant, ϕ_{L1} is the limit of integration which equals one of the roots of $P(\phi)$ and ϕ_{L2} is the other limit of integration, is suitable for this purpose. For the sake of convenience, we set $\delta=(\phi_M-\phi_{L1})/(\phi_M-\phi_B)$, $\phi_{L1}=\phi_B$ for the second integral and $\phi_{L1}=\phi_A$ for the third integral. Both alternatives are the same for the first integral. Eq. (A.12) becomes

$$\begin{aligned}I=2(\phi_M-\phi_B)^{-1/2}[&(a+b\phi_B+c/\phi_A)\mathscr{F}\\&+\tfrac{1}{3}(\phi_A-\phi_B)((c/\phi_A^2)k^2\mathscr{J}+b\mathscr{D})],\end{aligned}$$

where

$$k^2=(\phi_M-\phi_A)/(\phi_M-\phi_B),\quad \mathscr{F}=R_F(0,k^2,1),$$

$$\mathscr{D}=R_D(0,k^2,1),\quad \mathscr{J}=R_J\left(0,k^2,1,k^2\frac{\phi_B}{\phi_A}\right).$$

Turning back to the remaining terms defining V_{ell} in Eq. (A.3), the integrals of both A_{OPQ} and A_{Rh} can also be expressed as an analytical term plus an elliptic integral of the same type as Eq. (A.12), differing only in the values of the constants a,b,c. The contribution from A_{OPQ} needs first to be integrated by parts, while the integral of A_{Rh} does not.

The degenerated case $R_p=(r+r_c)$ (i.e. $\phi_S=\phi_A=1$) arises because $\sqrt{P(\phi)}$ becomes $(1-\phi)\sqrt{(\phi-\phi_B)}$. Then, Eq. (A.8) or (A.12) is no longer an elliptic integral, and it can be integrated analytically.

The evaluation of A and S can be carried out from geometrical concepts, as done for V. The expression for DA is evaluated from the definition $\mathrm{DA}=\mathrm{d}A/\mathrm{d}r$. The best stage to carry out this differentiation is from the primary expression of A, i.e. the equivalent expression to that in Eq. (A.5) for V. In all cases an equation like Eq. (A.12) also arises, but with different values of a,b,c.

The integral Vt (Eq. (2a)) is evaluated as follows. The term θ of V (Eq. (5a)) is integrated directly. There remains the term E_V corresponding to the elliptic integrals. The contribution from each body defined in Fig. (A.2) is individually undertaken. Consider, for instance, Eq. (A.6) for $V_{\mathrm{O'PQ}}$ with I defined in Eq. (A.8) and ϕ_B, ϕ_S and Δ defined with variable s substituting r_c. Once I is multiplied

by $(s\,\mathrm{d}s)$ and formally integrated over $0 < s < r_c$, the result can be interpreted as the integral of $\mathscr{R}(\phi,s)/\sqrt{P(\phi,s)}$ on a certain region of the plane (ϕ,s). The integration on variable s can be carried out first in an analytical way and the second step, integration on ϕ, leads to the result in terms of elliptic integrals. The procedure is repeated for the remaining contributions to V.

The expression for the integral At (Eq. (2b)) is obtained similarly.

All expressions given in Table 1 and Table 2 (Case 3) were checked by numerical integration of the primary integrals, like that defined in Eq. (A.3).

Appendix B.

Some specific features concerning the behavior of functions $E(r,r_c)$ defined in Table 1 of the main text will be pointed out here.

The limiting values for E_V, E_A, E_{Vt} and E_{At} are zero when both r, $r_c \to 0$, but the general expressions in Table 1 cannot be used as they stand. Instead, E_S and E_{DA} are non-zero and Table 1 may be used. For the sake of uniformity, all the values at $r = r_c = 0$ were listed in Table 2 as the particular Case 2.

For $(r_c + r) = R_p$ (Case 3), the general expressions in Table 1 should not be employed either. In particular, the second argument k^2 of the standard elliptic integrals defined in Table 1 becomes zero in this case. For computation purposes, it can be checked if k^2 becomes less than a tiny number to define Case 3. This number could be taken as the lower tolerance in the routines for the elliptic integrals, which is related to the machine underflow limit. However, a value as "high" as 10^{-25} can be directly taken without impairing the precision of the calculations. The limiting expressions for Case 3 are given in Table 2, where it is noted that $E_{\mathrm{DA}}(r,r_c)$ tends to infinity. In consequence, it should not be computed.

As the formulation in Table 1 can be employed down to a very small number of k^2, instead of computing Case 3 with the exact formulation given in Table 2, $k^2 = 10^{-25}$ can be set and Table 1 employed. The error will be negligible.

Following the definition of the coefficient γ in Table 1, the third kind of elliptic integral R_J ($R_J \equiv \mathscr{J}$ in Table 1) appears in functions E_V, E_A, E_{Vt} and E_{At}, but not in $E_S(r,r_c)$ and $E_{\mathrm{DA}}(r,r_c)$.

For E_V and E_A ($\gamma = \Delta$), the term $\mathscr{Z}_J$ in Table 1 becomes $\mathscr{Z}_J \propto (R_J\Delta)$ when $\gamma \neq 0$, i.e. when $r_c \neq r$. The product $(R_J\Delta)$ exhibits a jump at $r_c = r$ as $\Delta \to 0$ and $R_J \to \infty$ (its fourth argument $p = k^2(\phi_B/\phi_A) = 0$, because $\phi_B = 0$). The proper value of the term $\mathscr{Z}_J$ at $r_c = r$ can be found if this condition is set before carrying out the integration which leads to the general expressions in Table 1. It turns out that the value $\mathscr{Z}_J = 0$ should be assigned when $r_c = r$ (i.e. when $\gamma = 0$), as pointed out in Table 1. The behavior thus defined for $\mathscr{Z}_J$ is such that it counterbalances the step function $\theta(r,r_c)$ (Eq. (6) in the main text), allowing a smooth behavior for $V(r,r_c)$ and $A(r,r_c)$.

For E_{Vt} and E_{At}, $\mathscr{Z}_J \propto (R_J\Delta^2)$ shows a ramp at $r_c = r$ with the limit $\mathscr{Z}_J = 0$. This behavior exactly counterbalances the term $\Gamma(r,r_c)$ (Eq. (8) in the main text), allowing a smooth behavior for both $\mathrm{Vt}(r,r_c)$ and $\mathrm{At}(r,r_c)$.

For computation purposes, the condition $r \approx r_c$ can be practically detected when the parameter p becomes less than a tiny number (as commented on above, 10^{-25} is adequate), the case in which $\mathscr{Z}_J = 0$ and $\theta = \pi/2$ (for V and A) should be simultaneously taken.

It is interesting to note that at $|r_c - r| = R_p$, just when the intersection between the sphere and the cylindrical surface reduces to a point, the functions $E(r,r_c)$ become zero with the exception of $E_{\mathrm{DA}} = (\pi/4)\,R_p/(r - r_c)^{1/2}$. This means that $\mathrm{DA}r(r,r_c)$ drops from a finite value to zero once $|r_c - r|$ becomes just larger than R_p.

If desired, the Carlson standard elliptic integrals R_F, R_D and R_J defined in Table 1 can be readily converted to the Legendre standard elliptic integral by using the formulation given in Press et al. (1992).

References

Benenatti, R. F., & Brosilov, C. B. (1962). Void fraction distribution in bed of spheres. *American Institute of Chemical Engineers Journal*, *8*(3), 359–361.

Bey, O., & Eigenberger, G. (1997). Fluid flow through catalyst filled tubes. *Chemical Engineering Science*, *52*, 1365–1376.

Cybulski, A., Eigenberger, G., & Stainkiewicz, A. (1997). Operational and structural nonidealities in modelling and design multitubular catalytic reactors. *Industrial and Engineering Chemistry Research*, *36*, 3140–3148.

Delmas, H., & Froment, G. F. (1988). A simulation model accounting for structural radial nonuniformities in fixed beds reactors. *Chemical Engineering Science*, *43*, 2281–2287.

Dixon, A. G., & Welch, G. J. (1987). A structure-based model for heat transfer in low d_t/d_p fixed-bed reactor tubes. Presented at the *American Institute of Chemical Engineers Annual Meeting*, New York, USA.

Giese, M., Rottschäfer, K., & Vortmeyer, D. (1998). Measured and modelled superficial flow profiles in packed beds with liquid flow. *American Institute of Chemical Engineers Journal*, *44*, 484–490.

Govindarao, V. M. H., & Froment, G. F. (1986). Voidage profiles in packed beds of spheres. *Chemical Engineering Science*, *41*, 533–539.

Govindarao, V. M. H., & Ramrao, K. V. S. (1988). Prediction of location of particles in the wall region of a randomly packed bed of spheres. *Chemical Engineering Science*, *43*, 2544–2545.

Govindarao, V. M. H., Ramrao, K. V. S., & Rao, A. V. S. (1992). Structural characteristics of packed beds of low aspect ratio. *Chemical Engineering Science*, *47*, 2105–2109.

Kubie, J. (1988). Influence of containing walls on the distribution of voidage in packed beds of uniform spheres. *Chemical Engineering Science*, *43*, 1403–1405.

Küfner, R., & Hofmann, H. (1990). Implementation of radial porosity and velocity distribution in a reactor model for heterogeneous catalytic gas-phase reactions (torus-model). *Chemical Engineering Science*, *45*, 2141–2146.

Legawiec, B., & Ziólkowski, D. (1994). Structure, voidage and effective thermal conductivity of solids within near-wall region of beds packed with spherical pellets in tubes. *Chemical Engineering Science*, *49*, 2513–2520.

Mariani, N. J., Mazza, G. D., Martínez, O. M., & Barreto, G. F. (1998). The distribution of particles in cylindrical packed beds. *Trends in Heat, Mass & Momentum Transfer*, *4*, 95–114.

Mariani, N. J., Mazza, G. D., Martínez, O. M., & Barreto, G. F. (2000). Evaluation of radial voidage profile in packed beds of low aspect ratios. *The Canadian Journal of Chemical Engineering*, *78*, 1133–1137.

Mueller, G. E. (1992). Radial void fraction distributions in randomly packed fixed beds of uniformly sized spheres in cylindrical containers. *Powder Technology*, *72*, 269–275.

Mueller, G. E. (1999). A radial void fraction correlation for packed bed tubes. *The Canadian Journal of Chemical Engineering*, *77*, 132–135.

Papageorgiou, J. N., & Froment, G. F. (1995). Simulation models accounting for radial voidage profiles in fixed-bed reactors. *Chemical Engineering Science*, *50*, 3043–3056.

Press, W. H., Teukolsky, S. A., Vetterling, W. T., & Flannery, B. P. (1992). *Numerical recipes in Fortran* (2nd ed.). Cambridge, United Kingdom: Cambridge University Press.

Ridgway, K., & Tarbuck, K. J. (1968). Voidage fluctuations in randomly-packed beds of spheres adjacent to a containing wall. *Chemical Engineering Science*, *23*, 1147–1155.

Singleton, F. D. (1971). *Dispersion of mass in packed beds*. Ph.D. dissertation, University of Rochester.

Subagyo, S., Standish, N., & Brooks, G. A. (1998). A new model of velocity distribution of a single-phase fluid flowing in packed beds. *Chemical Engineering Science*, *53*, 1375–1385.

Toye, D., Marchot, P., Crine, M., Pelsser, A. M., & L'Homme, G. (1998). Local measurements of void fraction and liquid holdup in packed columns using X-ray computed tomography. *Chemical Engineering and Processing*, *37*, 511–520.

Winterberg, M., Tsotsas, E., Krischke, A., & Vortmeyer, D. (2000). A simple and coherent set of coefficients for modelling of heat and mass transport with and without chemical reaction in tubes filled with spheres. *Chemical Engineering Science*, *55*, 967–979.